DOI: 10.1002/chem.201001434

A Series of Vanadogermanates from 1D Chain to 3D Framework Built by Ge–V–O Clusters and Transition-Metal-Complex Bridges

Jian Zhou,[a, c] Jie Zhang,[a] Wei-Hui Fang,[a] and Guo-Yu Yang*[a, b]

Abstract: Three novel extended vanadogermanates, $\{[(en)_2Cd_2Ge_8V_{12}O_{40}(OH)_8(H_2O)][Cd(en)_2]_2\}\cdot 6H_2O$ (**1**), $\{[Zn_2(dap)_3][Zn(dap)]_2Ge_6V_{15}O_{48}(H_2O)\}[Zn(dap)_2(H_2O)]_2\cdot 3H_2O$ (**2**), and $\{[Cd_3(\mu\text{-dien})_2(Hdien)_2(H_2O)_2]Ge_4V_{16}O_{42}(OH)_4(H_2O)\}\cdot 2H_2O$ (**3**; en = ethylenediamine, dap = 1,2-diaminopropane, dien = diethylenetriamine), have been hydrothermally synthesized and structurally characterized by elemental analysis, IR spectroscopy, powder XRD, thermogravimetric analysis, and single-crystal XRD. Their Ge–V–O cluster anions are derived from the $V_{18}O_{42}$ cluster shell by replacing VO_5 square pyramids with Ge_2O_7 groups. Compound **1** exhibits a 1D sinusoidal chain built up from rare inorganic–organic hybrid dicadmium-substituted vanadogermanate $\{[Cd(en)]_2V_{12}O_{40}(GeOH)_8(H_2O)\}$ clusters and $[Cd(en)_2]$ complexes. Compound **2** is the first example of a 2D network based on linkage of the unusual $\{Ge_6V_{15}O_{48}(H_2O)\}$ clusters and two types of Zn complex fragments. Compound **3** is an unprecedented 3D framework built by $\{Ge_4V_{16}O_{42}(OH)_4(H_2O)\}$ clusters and rare trinuclear bridging complex cations $[Cd_3(\mu\text{-dien})_2(Hdien)_2(H_2O)_2]^{8+}$. Magnetic measurements illustrate that both **1** and **2** have antiferromagnetic exchange interactions between metal centers, whereas **3** exhibits ferrimagnetic behavior, which is rare in polyoxovanadate complexes.

Keywords: germanium · hydrothermal synthesis · magnetic properties · polyoxometalates · vanadium

Introduction

The significant interest in polyoxometalates (POMs) is due to wide structural variety combined with interesting properties in catalysis, materials science, and medicine.[1] A promising approach to make novel polyoxoanions is incorporation of other heteroatoms into cages composed of early transition metals. Many different elements have been reported as constituents of heteropolyanions,[2] and POMs containing heteroatoms inspire an enormous amount of new research due to their intriguing range of applications, which are manifested in a growing number of publications concerning this field.[3] These heteropolyoxoanions are an outstanding class of inorganic building blocks, which can be further connected with various transition-metal complexes (TMCs) as bridging ligands through covalent bonds to give a new class of extended POM-based materials with novel structures and unusual properties.[4] To date, a number of extended POM-based frameworks have been reported, as exemplified by 1D straight chain $\{[Cd(en)_2]_2[(en)_2Cd_2As_8V_{12}O_{40}]\}_n$ constructed from $[(en)_2Cd_2As_8V_{12}O_{40}]^{4-}$ cages and $[Cd(en)_2]^{2+}$ complex units,[5] a 2D network built by double-Dawson-type $[\alpha_1\text{-}CuP_2W_{17}O_{60}(OH)]_2^{14-}$ clusters and $[Cu(en)_2]^{2+}$ bridging units,[6] and 3D (3,6)-connected nets with $(4\cdot6^2)\cdot(4^2\cdot6^4\cdot8^7\cdot10^2)$ topology assembled from octa-Cu sandwiched $[Cu^{II}_8(en)_4(H_2O)_2(B\text{-}\alpha\text{-}SiW_9O_{34})_2]^{4-}$ POM clusters and $\{Cu(H_2O)_2\}$ bridging groups.[4b] Notably, the reported extended POM-based frameworks are usually joined by mononuclear complexes with octahedral or trigonal-bipyramidal configuration as linkers.[1d,4–6] However, no extended POMs containing multinuclear (e.g., bi- and trinuclear) complex linkers have been documented until now, to the best of our knowledge.

[a] Dr. J. Zhou, Prof. Dr. J. Zhang, W.-H. Fang, Prof. Dr. G.-Y. Yang
State Key Laboratory of Structural Chemistry
Fujian Institute of Research on the Structure of Matter
Chinese Academy of Sciences
Fuzhou, Fujian 350002 (P.R. China)
Fax: (+86) 591-83710051
E-mail: ygy@fjirsm.ac.cn

[b] Prof. Dr. G.-Y. Yang
MOE Key Laboratory of Cluster Science
Department of Chemistry, Beijing Institute of Technology
Beijing 100081 (P.R. China)
Fax: (+86) 10-68918572
E-mail: ygy@bit.edu.cn

[c] Dr. J. Zhou
Department of Chemistry and Biology, Yulin Normal University
Yulin, Guangxi 537000 (P.R. China)

Supporting information for this article is available on the WWW under http://dx.doi.org/10.1002/chem.201001434.

Thus, the use of multinuclear complex linkers for making extended POMs is a great challenge.

Of the POMs, polyoxovanadates (POVs) are a fascinating family of metal oxides because of their various coordination geometries and strong tendency to offer mixed-valent states. Therefore, POV clusters are suitable for the design of new POV-based materials with novel electronic, magnetic, and topological properties.[7] Recently, intense research on POVs mainly focused on the incorporation of group 15 elements (As and Sb) into the cage of the $\{V_{18}O_{42}\}$ cluster. Since the first As–V–O cluster $[As_6V_{15}O_{42}(H_2O)]^{6-}$ was prepared by Müller and Döring in 1988,[7a] a large number of As–V–O and Sb–V–O clusters with general formula $[M_{2n}V_{18-n}O_{42}(X)]$ (M = As, Sb; n = 2, 3, 4; X = H_2O, Cl^-, SO_3^{2-}) have been synthesized by many groups by different methods in solution, as exemplified by $Na_4[V^{IV}{}_8V^{V}{}_4As_8O_{40}(H_2O)]\cdot 23H_2O$,[7d] $[M(bbi)_2]_2[As_8V_{14}O_{42}(H_2O)]$ (M = Co, Ni, Zn; bbi = 1,1′-(1,4-butanediyl)bis(imidazole)),[8] $[(H_2O)Zn(4,4'\text{-bpy})]_2[As_8V_{14}O_{42}(H_2O)]\cdot 2H_2O$ (bpy = 2,2′-bipyridine),[9] $(trenH_3)_2[V_{15}Sb_6O_{42}]\cdot 0.33\,tren\cdot n\,H_2O$ (tren = tris(2-aminoethyl)amine; n = 3–5),[10] and $[C_6H_{17}N_3]_4[Sb_4V_{16}O_{42}]\cdot 2H_2O$ ($C_6H_{17}N_3$ = 2-piperazine-*N*-ethylamine).[11] Lately, we have explored the application of secondary TMCs as bridging units linking $[As_{2n}V_{18-n}O_{42}(X)]$ (n = 2, 3, 4; X = H_2O) clusters into many extended structures under hydrothermal conditions.[12] However, except for a few discrete vanadogermanates[13,7g] and two extended vanadosilicates including a 1D chain $Cs_{10.5}[(V_{16}O_{40})(Si_{4.5}V_{1.5}O_{10})]\cdot 3.5H_2O$[7f] and a 3D framework $[H_4V_{18}O_{46}(SiO)_8(DAB)_4(H_2O)]\cdot 4H_2O$ (DAB = $NH_2(CH_2)_4NH_2$),[7e] no systematic investigation of the related POVs incorporating group 14 elements, that is, Si(Ge)–V–O clusters, have been carried out under hydrothermal conditions.

Furthermore, it is expected that the second TMs can further be incorporated into POV backbones, which may not only generate a new class of materials with novel framework topology but also lead to new properties. However, few investigations have been carried out on TM-substituted POVs because it is hard to obtain lacunary POV precursors, compared with abundant TM-substituted polyoxotungstates.[14] Therefore, we initiated an exploration of the As–V–O synthetic system in the presence of second TM ions under hydrothermal conditions with the aim of obtaining TM-substituted POVs. Accordingly, we have successfully made a series of mono- and di-TM-substituted As–V–O clusters (TM = Ni, Zn, Cd).[5,15] Later, similar conditions were employed by Wang and co-workers to make some Zn/Cd-substituted As–V–O clusters with mixed organoamine ligands.[16] In contrast, TM-substituted Si(Ge)–V–O clusters are rare. As part of our ongoing work, we further extended our interest from the As–V–O and TM-substituted As–V–O clusters to Ge–V–O and TM-substituted Ge–V–O clusters under hydrothermal conditions based on the following considerations: 1) the $\{As^{III}{}_2O_5\}$ units of the As–V–O cage are not useful for making extended structures because the electron lone pairs of the As^{III} atoms effectively terminate the structure, whereas the $\{Ge^{IV}{}_2O_7\}$ units of the Ge–V–O cage can provide an opportunity for making extended structures because the Ge^{IV} atoms have diverse coordination geometries of tetrahedron, square pyramid, and octahedron. 2) Like the As–V–O clusters, the V=O groups of the Ge–V–O cluster should also be substitutable by TM complexes to give new inorganic–organic hybrid clusters. As expected, three extended vanadogermanates, including a TM-substituted 1D chain $\{[(en)_2Cd_2Ge_8V_{12}O_{40}(OH)_8(H_2O)][Cd(en)_2]_2\}\cdot 6H_2O$ (**1**), a 2D network $\{[Zn_2(dap)_3][Zn(dap)]_2Ge_6V_{15}O_{48}(H_2O)\}[Zn(dap)_2(H_2O)]_2\cdot 3H_2O$ (**2**), and a TMC-bridged 3D framework $\{[Cd_3(\mu\text{-dien})_2(Hdien)_2(H_2O)_2]Ge_4V_{16}O_{42}(OH)_4(H_2O)\}\cdot 2H_2O$ (**3**), were made under hydrothermal conditions. Compound **1** is the first 1D dicadmium-substituted vanadogermanate built by $Cd_2Ge_8V_{12}O_{40}(OH)_8(H_2O)$ clusters and TMC bridges, whereas **2** and **3** are the first 2/3D vanadogermanates constructed from $Ge_6V_{15}O_{48}(H_2O)$/$Ge_4V_{16}O_{42}(OH)_4(H_2O)$ clusters and polynuclear TMC linkers.

Results and Discussion

Synthesis and IR spectra: Hydrothermal synthesis has recently been proven to be a powerful technique in the preparation of organic–inorganic hybrid materials in the POM field because hydrothermal conditions can cause a reaction to shift from the kinetic to the thermodynamic domain and overcome difficulties due to differential solubilities of organic and inorganic starting materials.[17] In a specific hydrothermal process, many factors, such as the type of initial reactants, pH value, temperature, solvents, quantity of solvent, reactant stoichiometry, reactant concentration, and reaction time, can influence the outcome of reaction. For instance, black crystals of **1** were obtained in high yield in the presence of H_3BO_3. With the aim of preparing an analogue of **1**, we tried to replace en with dap alone, but these attempts failed. When Zn^{2+} ions replace the Cd^{2+} ions of the above reaction system in the absence of H_3BO_3, black crystals of **2** containing unusual dinuclear $[Zn_2(dap)_3]^{4+}$ bridging groups were isolated. Subsequently, to further investigate the influence of organic amines on the structure of the products, the synthetic procedure used for making **2** was modified by replacing dap with dien, which afforded novel 3D vanadogermanate **3** with a rare trinuclear $[(H_2O)(Hdien)Cd(\mu\text{-dien})Cd(\mu\text{-dien})Cd(Hdien)(H_2O)]^{8+}$ bridging group. These results demonstrated that the different organic amines have a significant structure-directing effect on the formation of the different extended frameworks of **1**–**3**.

We studied the influence of synthetic parameters on the products: 1) pH value: The crystallization of **1**–**3** was found to be highly sensitive to the pH of the reaction mixture, which was controlled at pH 10.0 to 10.5 for **1**, pH 12.0 to 12.5 for **2**, and pH 8.8 to 9.0 for **3**, and no crystalline product could be obtained outside these pH ranges. 2) Reactant stoichiometry: The molar ratio of the reactants plays a vital role in the formation of **1**. Only when the Ge/V molar ratio was equal to or slightly less than 1:2 was **1** produced. Otherwise, a red amorphous phase was isolated. However, crystallization seems not to be related to the Ge/V molar ratio for

2 and **3**, which were the only product under similar reaction conditions, but when the quantity of Cd or Zn was increased to two- or threefold with the other parameters kept unchanged, a black amorphous product was isolated. 3) Solvent: Ethylene glycol as a reaction medium is suitable for the crystal growth of **3**. Attempts to synthesize **3** by using other organic solvents, such as ethanol, pyridine, and *N*,*N*-dimethylformamide, were unsuccessful. Moreover, we also found that the Ge–V–O system is not sensitive to reaction temperature. The expected crystals were also formed when the reaction temperature was adjusted 10 °C above or 20 °C below 170 °C. For **1**, **2**, and **3**, good accordance between the experimental and simulated powder XRD patterns indicates phase purity of the samples (Figure 1).

The IR spectra of **1**–**3** were recorded between $\tilde{\nu}=4000$ and 400 cm^{-1} (Figure S1, Supporting Information). The stretching bands of NH_2 and CH_2 groups are observed at $\tilde{\nu}=$ 3312 to 3331 and 2881 to 2939 cm^{-1}, respectively, and their bending bands at $\tilde{\nu}=1579$ to 1598 and 1338 to 1455 cm^{-1}, respectively. These signals confirm the presence of amino groups in **1**–**3**. The broad band at $\tilde{\nu}=3427$ to 3465 cm^{-1} can be assigned to OH stretching. The strong peaks at $\tilde{\nu}=957$ to 986 cm^{-1} can be attributed to the stretching vibrations of V=O bonds, whereas the strong peaks at $\tilde{\nu}=718$ to 813 cm^{-1} may be due to asymmetric GeO stretching of the GeO_4 tetrahedra.

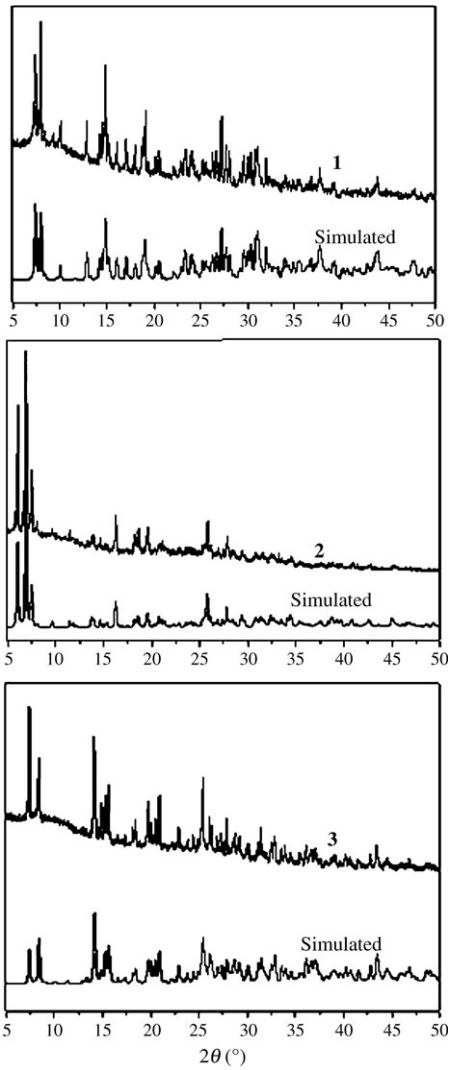

Figure 1. Simulated and experimental powder XRD patterns of compounds **1**–**3**.

Structural description

{[(en)$_2$Cd$_2$Ge$_8$V$_{12}$O$_{40}$(OH)$_8$(H$_2$O)][Cd(en)$_2$]$_2$}·6H$_2$O (***1***): The molecular structure of **1** consists of a di-Cd-substituted Ge–V–O cluster [(en)$_2$Cd$_2$Ge$_8$V$_{12}$O$_{40}$(OH)$_8$(H$_2$O)] ($Cd_2Ge_8V_{12}$), two $[Cd(en)_2]_2$ supporting groups, and seven lattice water molecules. As shown in Figure 2, an unusual feature of **1** is that two $Cd(en)^{2+}$ fragments take the place of two VO^{2+} groups located between the Ge_2O_7 units of the reported $Ge_8V_{14}O_{50}$ cage with rhombicuboctahedral topology,[7e] forming a new $Cd_2Ge_8V_{12}$ cluster. Each $Cd_2Ge_8V_{12}$ unit is further decorated by two $[Cd(en)_2]^{2+}$ units to generate the unprecedented cluster {[(en)$_2$Cd$_2$Ge$_8$V$_{12}$O$_{40}$(OH)$_8$(H$_2$O)][Cd(en)$_2$]$_2$} (Figure 2a and b). In compound **1**, three unique Cd sites display two different coordination environments: $N_2Cd(1,2)O_4$ trigonal prisms and distorted $OCd(3)N_4$ square pyramids. The former is composed of two N atoms of one en ligand (Cd–N 2.288(10)–2.340(7) Å) and four bridging O atoms

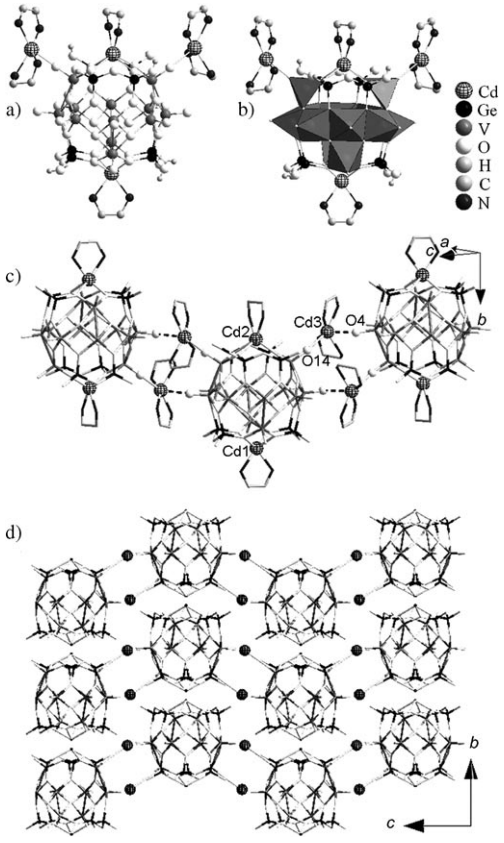

Figure 2. a), b) Ball-and-stick/polyhedral representations of the cluster in **1**. c) 1D extended chain constructed by weak Cd···O interactions. d) 1D sinusoidal chains arranged in parallel. All en ligands are omitted for clarity.

from four adjacent VO_5 groups (Cd–O 2.285(6)–2.370(5) Å), and the latter is defined by four N atoms of two en ligands (Cd–N 2.270(8)–2.326(8) Å) and one O atoms from the neighboring VO_5 group (Cd–O 2.411(5) Å). All V centers have a distorted VO_5 square-pyramidal environment. The V–O distances of these terminal O atoms range from 1.604(3) to 1.620(3) Å, whereas those for the basal, shared O atoms range from 1.912(3) to 2.006(3) Å. The V···V distances range from 2.8573(11) to 3.0341(13) Å. In the Ge_2O_7 fragments, the Ge–O distances vary from 1.716(3) to 1.779(3) Å. On the basis of bond valence sum calculations,[18] the oxidation state of all V atoms in **1** is +4 (4.08–4.14), and that of the eight Ge atoms is +4 (3.97–4.09). Presumably, the Cd and O atoms have their usual valences of +2 and −2, respectively. In addition, the bond valence sums for terminal O18, O21, O23, and O24 atoms on the Ge atoms in **1** are less than 1, which suggests that these O atoms belong to OH groups. Similar OH groups have also been reported in other Ge–V–O clusters, such as $(H_2dab)_4[V_{14}O_{44}(GeOH)_8]\cdot 6H_2O$ (dab = 1,4-diaminobutane),[7e] $Cs_8[V_{16}O_{42}(GeOH)_4]\cdot 4.7H_2O$, and $K_5V_{12}O_{40}(GeOH)_8(SO_4)\cdot 10H_2O$.[13]

It is interesting that the Cd3 atom also has significant weak Cd–O interactions of 2.856(3) Å, which is shorter than the sum of the van der Waals radii (< 3.7 Å).[19] The relatively long Cd–O bonds may be a consequence of steric interactions between the en ligands and the $Cd_2Ge_8V_{12}$ clusters. Thus, the adjacent $Cd_2Ge_8V_{12}$ clusters are further linked by a pair of bridging $[Cd(en)_2]^{2+}$ groups to form a rare 1D hybrid sinusoidal chain in the Ge–V–O system (Figure 2c). All such chains are arranged in parallel with an interchain distance of about 10.65 Å (Figure 2d) and further through N–H···O and O–H···O hydrogen bonds between POVs, resulting in a 3D supramolecular framework with pseudocircular channels along the *c* axis (Figure S2, Supporting Information), in which the coordinated en molecules are located. The N–H···O distances vary from 2.11 to 2.41 Å, and the N–H···O angles from 113.1 to 165.2° (Table S2, Supporting Information). The O–H···O distances vary from 1.92 to 2.27 Å, and the O–H···O angles from 164.1 to 173.4°. These values are consistent with those reported in the literature.[5]

*Structure of {[$Zn_2(dap)_3$][$Zn(dap)$]$_2Ge_6V_{15}O_{48}(H_2O)$}[$Zn(dap)_2(H_2O)$]$_2\cdot 3H_2O$ (**2**)*: The structure of **2** consists of 2D $\{[Ge_6V_{15}O_{48}(H_2O)][Zn_2(dap)_3][Zn(dap)]_2\}^{4-}$ anionic layers, charge-compensating $[Zn(dap)_2(H_2O)]^{2+}$ cations, and lattice water molecules. The $[Ge_6V_{15}O_{48}(H_2O)]^{12-}$ unit in **2** is a new type of acentric Ge–V–O cage. It consists of fifteen VO_5 square pyramids and six GeO_4 tetrahedra, with one neutral H_2O molecule at the center (Figure 3a and b). Seven VO_5 square pyramids form a heptamer by sharing edges and corners. The heptamer and one Ge_2O_7 unit are joined together by sharing O atoms to form a circular $V_7Ge_2O_{19}$ unit. Three VO_5 square pyramids share edges to produce a trimer. Two trimers, one located on top and one at the bottom of the circular $V_7Ge_2O_{19}$ unit, are rotated by 90° with respect to each other. The remaining four windows are capped by two Ge_2O_7 units and two VO_5 groups to give a cluster with the

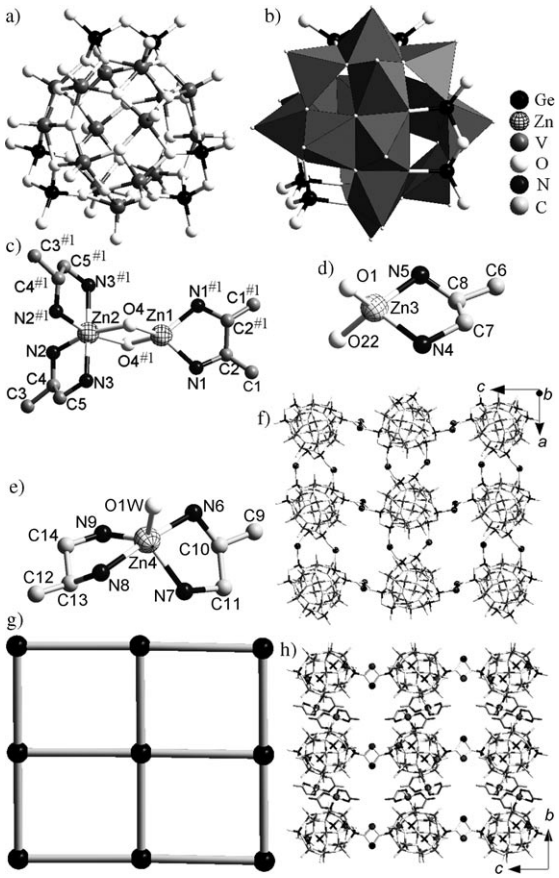

Figure 3. a), b) Ball-and-stick/polyhedral representations of the $[Ge_6V_{15}O_{48}(H_2O)]$ cluster in **2**. c) Structure of dinuclear bridging complex $[Zn_2O_2(dap)_3]$. Symmetry code for #1: $1-x$, y, $-0.5-z$. d) Structure of mononuclear bridging complex $[ZnO_2(dap)]$. e) Structure of isolated $[Zn(dap)_2(H_2O)]^{2+}$ cations. f) View of linkages of the 2D layer in **2** (all dap ligands are omitted for clarity). g) Network topology of **2** (spheres: $[Ge_6V_{15}O_{48}(H_2O)]$ clusters). h) Isolated $[Zn(dap)_2(H_2O)]^{2+}$ cations located between the layers in **2**.

overall chemical composition of $[Ge_6V_{15}O_{48}(H_2O)]^{12-}$. In the VO_5 pyramids of **2**, the V–O bonds corresponding to the basal plane vary from 1.919(4) to 2.069(5) Å, whereas the shorter V–O bond distances ranging from 1.612(5) to 1.637(5) Å correspond to the axial V=O bonds of the VO_5 pyramids. The Ge–O bonds of the Ge_2O_7 units are in the range of 1.724(6)–1.809(5) Å. The assignment of oxidation states for the Ge and V atoms is confirmed by bond valence sums,[18] which give average valences of 3.85 and 3.89 for Ge and V, respectively.

Interestingly, there are two types of unusual bridging TMCs in **2**. One is the dinuclear bridging $[Zn_2O_2(dap)_3]$ group (Figure 3c) formed by connection of $[Zn(dap)]^{2+}$ and $[Zn(dap)_2]^{2+}$ cations through two bridging O atoms from $[Ge_6V_{15}O_{48}]^{12-}$ units. The Zn···Zn separation is 3.12 Å. It is worth noting that the tetrahedral bridging $[Zn(dap)]^{2+}$ cation and dinuclear bridging $[Zn_2(dap)_3]^{4+}$ cation have not been reported to date, because dap-based TMCs generally adopt a distorted octahedral $[TMO_2(dap)_2]$ bridging mode.[20] The other is the mononuclear bridging $[Zn(dap)]^{2+}$ cation, which also adopts a tetrahedral bridging mode to

link $[Ge_6V_{15}O_{48}]^{12-}$ units (Figure 3d). In addition, the Zn atoms in the isolated charge-compensating $[Zn(dap)_2(H_2O)]^{2+}$ cations (Figure 3e) adopt a distorted square-pyramidal geometry comprised of four N atoms of two en ligands and one water molecule.

As shown in Figure 3f, the $[Ge_6V_{15}O_{48}(H_2O)]^{12-}$ clusters are interconnected to form a 1D straight chain along the *a* axis through a pair of $[Zn(dap)]^{2+}$ bridging groups. These chains are further linked by dinuclear $[Zn_2(dap)_3]^{4+}$ bridging groups along the *c* axis to generate a 2D network within the *ac* plane. Each terminal O4 atom of GeO_4 tetrahedra binds to two Zn(1,2) atoms along the *c* axis in an uncommon μ_3-O4 coordination mode, which is different from the terminal O atoms linking the Mo(V,W) atoms of other POMs as bridging ligand that usually displays the μ_2-O coordination mode.[20] The network topology of the 2D layered anion can be simplified by considering the $[Ge_6V_{15}O_{48}(H_2O)]^{12-}$ units as nodes, and $[Zn(dap)]^{2+}$ and $[Zn_2(dap)_3]^{4+}$ groups as linkers between the cluster nodes, and thus the structure displays 2D (4,4)-network topology with Schläfli symbol of $4^4{\cdot}6^2$ and the vertex symbol or long symbol of 4·4·4·4 (Figure 3g). The $[Zn(dap)_2(H_2O)]^{2+}$ cations are arranged as a straight chain along the *a* axis. These cationic chains are sandwiched between the anionic layers stacked along the *b* axis in AAA sequence with an interlamellar separation of approximately 8.03 Å (Figures 3h and S3, Supporting Information), generating pseudo 1D channels along the *a* axis in which the lattice water molecules are located.

Generally, 2D layered POVs are joined by the same TMC linkers,[20b,c] and to date only a few examples are linked by different TMC linkers, such as $[Co(en)_2][Co(bpy)_2][PMo^{VI}{}_5Mo^{V}{}_3V^{IV}{}_8O_{44}]\cdot 4.5H_2O$ (**4**)[4d] and $[Cd(dien)]_2[Cd(dien)(H_2O)]_2[As_4V_{16}O_{42}(H_2O)]\cdot 2H_2O$ (**5**).[21] In **4**, double $[Co(bpy)_2]$ bridges connect $[PMo^{VI}{}_5Mo^{V}{}_3V^{IV}{}_8O_{44}]$ clusters along the *a* axis, whereas the $[Co(en)_2]$ fragments link $[PMo^{VI}{}_5Mo^{V}{}_3V^{IV}{}_8O_{44}]$ clusters along the short diagonal of the *ab* plane. In **5**, the $[As_4V_{16}O_{42}(H_2O)]$ clusters are linked by a pair of $[Cd(dien)(H_2O)]$ bridges to form a 1D chain along the *a* axis, and the chains are further interconnected by another pair of [Cd(dien)] bridges along the *c* axis to generate a 2D neutral layer. Although 2D layered neutral networks in **4** and **5** are constructed by two types of mononuclear TMCs, the 2D layer in **2** based on mono- and dinuclear TMCs as the bridges is first of its kind, to the best of our knowledge.

Structure of {[Cd$_3$(μ-dien)$_2$(Hdien)$_2$(H$_2$O)$_2$]Ge$_4$V$_{16}$O$_{42}$(OH)$_4$(H$_2$O)}·2H$_2$O (**3**): Compound **3** consists of β-$[Ge_4V_{16}O_{42}(OH)_4]^{8-}$ cages and rare trinuclear bridging $[Cd_3(\mu\text{-dien})_2(Hdien)_2(H_2O)_2]^{8+}$ linkers. The β-$[Ge_4V_{16}O_{42}(OH)_4]$ cage (Figure 4a and b) in **3** is constructed from sixteen VO_5 square pyramids and four GeO_4 tetrahedra, with one neutral H_2O molecule at the center. Eight VO_5 square pyramids are linked together to form an equatorial eight-ring by edge sharing. Three VO_5 square pyramids share their opposite edges to form a trimer. Two trimers, one located on top and one at the bottom of the eight-ring, are rotated by about 45°

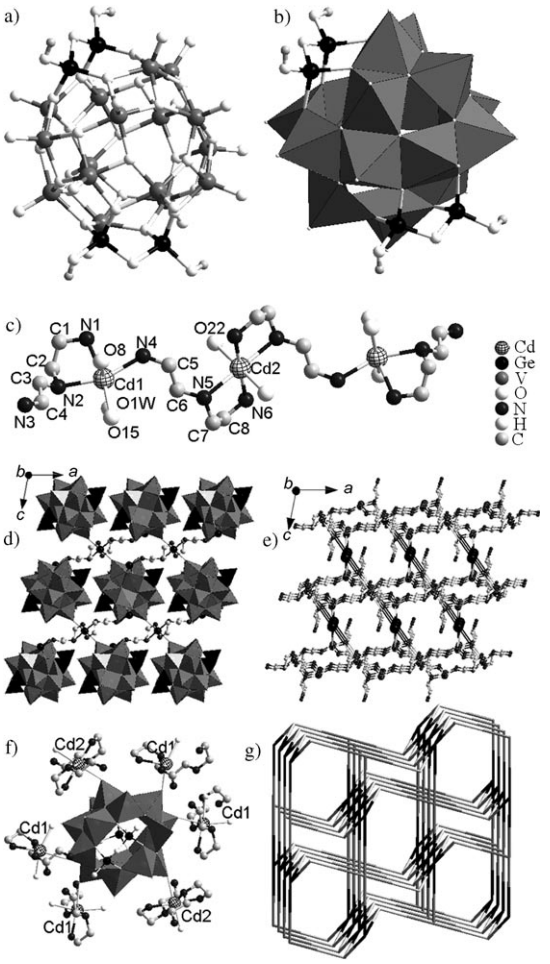

Figure 4. a), b) Ball-and-stick/polyhedral representation of β-$[Ge_4V_{16}O_{42}(OH)_4]$ cluster. c) Structure of trimeric bridging complex $[Cd_3(\mu\text{-dien})_2(Hdien)_2(H_2O)_2]$. d) Polyhedral view of the 3D framework formed by β-$[Ge_4V_{16}O_{42}(OH)_4]$ clusters and trimeric $[Cd_3(\mu\text{-dien})_2(Hdien)_2(H_2O)_2]$ bridging complexes. e) View of the 3D framework of **3**, showing the arrangement of trimeric $[Cd_3O_6(\mu\text{-dien})_2(Hdien)_2(H_2O)_2]$ bridging complexes (black atoms; *β*-$[Ge_4V_{16}O_{42}(OH)_4]$ cluster). f) View of the six-connecting mode of β-$[Ge_4V_{16}O_{42}(OH)_4]$ cluster. g) View of framework topology of **3**.

with respect to each other. Four GeO_4 groups form two pairs of Ge_2O_7 moieties through O bridges. The remaining four windows are capped by two Ge_2O_7 units and two VO_5 square pyramids to give a spherical Ge–V–O cluster of composition β-$[Ge_4V_{16}O_{42}(OH)_4]$. This cluster is similar to that in $Cs_8[Ge_4V_{16}O_{42}(OH)_4]\cdot 4.7H_2O$,[13] in which one of the Ge_2O_7 units and two VO_5 square pyramids are disordered over two positions. This disorder could be related to the weak interaction of Cs^+ cations and discrete Ge–V–O cluster anions. But both Ge_2O_7 units and VO_5 square pyramids in **3** are ordered, and this could result from the strongly coordinated interaction of TMC cations and Ge–V–O anions. On the basis of bond valence sum calculations,[18] the oxidation state of all V atoms in **3** is +4 (4.09–4.15), and that of the four Ge atoms +4 (4.03–4.05). The bond valence sums for terminal O atoms on the Ge atoms in **3** of less than 1 suggest that these O atoms belong to OH groups.

In the trinuclear $[Cd_3(\mu\text{-dien})_2(Hdien)_2(H_2O)_2]^{8+}$ (Cd_3) unit, two $[Cd(Hdien)]^{2+}$ moieties and one Cd^{2+} ion are joined by two dien bridges to form a centrosymmetric trimer (Figure 4c). There are two types of configurations for the dien molecule. In the first the dien molecule acts as bichelating ligand to bond the Cd1 atom, forming the $[Cd(Hdien)]^{2+}$ group, in which one N atom is protonated for charge balance. Here, the bicoordinated dien shows an unusual coordination mode. The dien molecules observed in related complexes usually act as strong trichelating ligands, for example, in $[Ni(dien)_2]_{0.5}[InS_2]$,[22] $[Ni(dien)_2]_2[Ge_7O_{13}(OH)_2F_3]Cl$,[23] and $[Co(dien)_2]_2[Sb_2Se_6]$.[24] In the second mode two N atoms of the bridging dien ligand coordinate to Cd2, whereas the third N atom coordinates to Cd1. This coordination mode is also unfamiliar; the only example is found in the dinuclear bridging $[(dien)Zn(\mu\text{-dien})Zn(dien)]^{4+}$ cation, which was recently reported by us.[12c] The TM ions are usually chelated by two tridentate amines to form saturated complexes with distorted octahedral coordination, which can not be further coordinated by the O atoms of the POM anion. Thus dien-based TMCs as bridging groups in POVs are relatively rare; the limited examples include mononuclear bridging $[Zn(dien)]^{2+}$,[25] dinuclear bridging $[(dien)Zn(\mu\text{-dien})Zn(dien)]^{4+}$ (which, in fact, is also a mononuclear bridging group, because one nonbridging $[Zn2(dien)]^{2+}$ complex is appended to a bridging $[Zn1(dien)]^{2+}$ fragment, linked through a tridentate μ-dien ligand),[12c] and a bridging trinuclear Cd_3 unit (this work). Reports on bridging groups have mainly focused on mononuclear $[TM(amine)_x]$ (amine = organic chelating amine) moieties to date. Although some unexpected binuclear $[TM_2(amine)_x]$ units have been observed in $\{[Zn(en)_2](\mu_2\text{-}en)[Zn(en)_2]\}^{4+}$,[26] $\{[Zn(dien)(H_2O)](\mu_2\text{-dien})[Zn(dien)(H_2O)]\}^{4+}$,[12c] and $\{[Zn(tren)](\mu_2\text{-teta})[Zn(tren)]\}^{4+}$ (teta = triethylenetetramine),[27] they just act as counterions to balance the charge, whereby the complex cations are centrosymmetric and the two TM sites display the same coordination environments. Although the trinuclear Cd_3 units in **3** have a symmetry center, the Cd sites display two kinds of different coordination environments: distorted octahedron ($Cd1N_3O_3$) with a *fac* configuration and distorted octahedron ($Cd2N_4O_2$) with a *trans* configuration. This unsaturated cation has not been reported until now, to the best of our knowledge. Therefore, the trinuclear Cd_3 unit in **3** is the only example of polynuclear bridging $[TM_n(amine)_x]$ ($n>2$) complex groups.

The structure of **3** is made up of β-$[Ge_4V_{16}O_{42}(OH)_4]$ cages linked by rare trinuclear bridging Cd_3 units into a novel 3D open framework (Figure 4d and e). As shown in Figure 4e, the trinuclear Cd_3 bridges are arranged along the *a* axis to form a pseudolayer in the *ab* plane. These pseudolayers are further stacked along the *c* axis in AAA sequence. Interestingly, the uncoordinated NH_2 groups of dien ligands, appended up and down the pseudolayers, are sandwiched between β-$[Ge_4V_{16}O_{42}(OH)_4]$ cages through N–H···O hydrogen-bonding interactions (N···O 2.922–2.999 Å). From a topological point of view, the structure of **3** is a 3D (3,4,6)-connected frameworks based on Cd1, Cd2 atoms and β-$[Ge_4V_{16}O_{42}(OH)_4]$ cages as 3-, 4-, and 6-connected nodes, respectively (Figure 4f). The Schläfli symbol for this net is $(6^3)(6^4{\cdot}8^2)(6^2{\cdot}8^4)$, and the long vertex symbol with rings is $(6{\cdot}6{\cdot}6)(6{\cdot}6{\cdot}6{\cdot}6{\cdot}8_2{\cdot}8_2)(6_2{\cdot}6_2{\cdot}8_3{\cdot}8_4{\cdot}8{\cdot}8_2)$ (Figure 4g). From the structural point of view, 3D framework **3** can also been described as a layer-pillared structure: each layer is built by β-$[Ge_4V_{16}O_{42}(OH)_4]$ and bridging Cd1 atoms, and then the adjacent layers are further linked by $Cd2(\mu\text{-dien})_2$ bridging groups as pillars (Figure S4, Supporting Information), forming the 3D framework (Figure 4d and e).

Structure relations of Ge–V–O and Si–V–O clusters derived from the $\{V_{18}O_{42}\}$ shell: The Ge–V–O and Si–V–O clusters with general composition $[Ge_{2n}V_{18-n}O_{42}(O,OH)_{2n}]$ or $[Si_{2n}V_{18-n}O_{42+2n}]$ are derived from the $\{V_{18}O_{42}\}$ cluster (Figure 5a) by replacing n VO_5 square pyramids with n M_2O_7

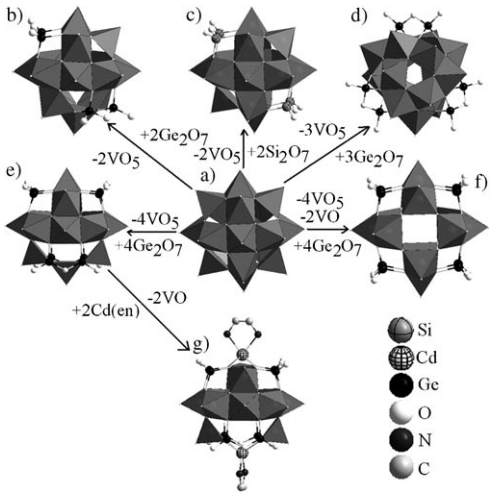

Figure 5. Structures of a) $[V_{18}O_{42}]$, b) $[Ge_4V_{16}O_{46}]$, c) $[Si_4V_{16}O_{46}]$, d) $[Ge_6V_{15}O_{48}]$, e) $[Ge_8V_{14}O_{50}]$, f) $[Ge_8V_{12}O_{48}]$, g) $[(en)_2Cd_2Ge_8V_{12}O_{48}]$.

groups (M = Si, Ge; n = 2, 3, 4). The β-$[Ge_4V_{16}O_{42}(OH)_4]$ cluster in **3** has D_2 symmetry and is the second example of the $[Ge_{2n}V_{18-n}O_{42}(OH)_{2n}]$ series with $n=2$ (Figure 5b). The β-$[Ge_4V_{16}O_{42}(OH)_4]$ cluster shows a relationship with α-$[Si_4V_{16}O_{46}]$ (Figure 5c) in $Cs_{10.5}[(V_{16}O_{40})(Si_{4.5}V_{1.5}O_{10})]\cdot 3.5H_2O$.[7f] The structure of β-$[Ge_4V_{16}O_{42}(OH)_4]$ can be derived from α-$[Si_4V_{16}O_{46}]$ by about 45° rotation of one-half of the α-$[Si_4V_{16}O_{46}]$ around the vertical axis of the equatorial eight-ring. Further replacement of one VO_5 square pyramid of cluster $[Ge_4V_{16}O_{42}(OH)_4]$ with one Ge_2O_7 group would result in the formation of cluster $[Ge_6V_{15}O_{48}]$. The $[Ge_6V_{15}O_{48}]$ cluster (Figure 5d) in **2** has D_3 symmetry and is the first example of the $[Ge_{2n}V_{18-n}O_{42}(O,OH)_{2n}]$ series with $n=3$. The Ge(Si)–V–O cluster with four M_2O_7 groups exhibits two types of conformation, namely, common α-$[M_8V_{14}O_{42}(O,OH)_8]$ (M = Ge, Si) cage with S_4 symmetry[7e,g,13] (Figure 5e) and unique β-$[Ge_8V_{12}O_{48}]$ cage of D_{4h} symmetry[13] (Figure 5f). The $[(en)_2Cd_2Ge_8V_{12}O_{42}(O,OH)_8]$ cluster (Figure 5g) in **1** derived from the α-$[Ge_8V_{14}O_{42}$-

$(O,OH)_8$] cluster displays D_{2d} symmetry and is a new member of the hybrid TM-substituted Ge–V–O cluster series. In addition, the $[Ge_6V_{15}O_{48}]$ unit of **2** has six GeO_4 tetrahedral corners available for further structural derivatives to readily form a layer. However, the related As–V–O clusters that are derived from the $\{V_{18}O_{42}\}$ shell by replacing VO_5 square pyramids with As_2O_5 groups cannot undergo further linking because the electron lone pairs on As^{III} effectively terminate the structure. Thus, it is reasonable to make a variety of 1-, 2-, and 3D POMs by using $[Ge_{2n}V_{18-n}O_{42}(O,OH)_{2n}]$ ($n=2,3,4$) clusters as structural building units.

Magnetic properties: The variable-temperature magnetic susceptibility of **1–3** was measured between 2 and 300 K. Figure S5 (Supporting Information) shows the magnetic behaviors of **1–3** in the form of the product $\chi_M T$ versus temperature, in which χ_M is the molar magnetic susceptibility. The $\chi_M T$ values for **1** and **2** at 300 K of 1.78 and 2.15 $cm^3 K mol^{-1}$, respectively, are much lower than the expected total spin-only value of 4.50 $cm^3 K mol^{-1}$ for 12 V^{4+} and 5.63 $cm^3 K mol^{-1}$ for 15 V^{4+} with $S=1/2$ ($g=2$) and thus indicate significant antiferromagnetic exchange interactions between V^{4+} ions in $Cd_2Ge_8V_{12}$ and the $[Ge_6V_{15}O_{48}(H_2O)]$ cluster. On cooling from room temperature, the $\chi_M T$ value falls steeply until about 150 K and then decreases steadily, reaching 1.41 $cm^3 K mol^{-1}$ at 25 K for **1**, and 1.09 $cm^3 K mol^{-1}$ at 20 K for **2**. Below these temperatures, another steeper decrease in $\chi_M T$ is observed. Such behavior is similar to that observed in $[(en)_2Cd_2As_8V_{12}O_{40}]$[5] and $[Zn_2(dien)_3]As_6V_{15}O_{42}(H_2O)]$.[12c] The short distances ($\leq$2.902 Å) between the V···V pairs with double O bridges (four pairs in **1** and six pairs in **2**) are in the range expected for strong antiferromagnetic coupling, and thus a low $\chi_M T$ value at high temperature results. The remaining vanadium ions are largely uncorrelated at high temperature. When the temperature is lowered further, weak antiferromagnetic couplings occur between these remaining vanadium centers, which correspond to the second decrease in **1** and **2**. The $\chi_M T$ values of 1.41 $cm^3 K mol^{-1}$ at 25 K and 1.09 $cm^3 K mol^{-1}$ at 20 K are in agreement with the calculated value for four and three uncoupled V^{4+} ions in **1** and **2**, respectively. For **3**, the $\chi_M T$ value of 2.97 $cm^3 K mol^{-1}$ is much smaller than the theoretical value (6.00 $cm^3 K mol^{-1}$) calculated for 16 isolated V^{4+}. Lowering the temperature decreases the $\chi_M T$ value to 1.69 $cm^3 K mol^{-1}$ at 50.0 K, which suggests the existence of dominant antiferromagnetic interactions between V^{4+} centers. Interestingly, an abrupt rise in the $\chi_M T$ value occurs on further cooling. This behavior is obviously relevant to the pronounced correlation of uncompensated spins, which is normally observed in ferrimagnetic systems.[28] From the structural data, it can be found that the two bis-oxo-bridged V1···V2 pairs within the β-$[Ge_4V_{16}O_{42}(OH)_4]$ cluster exhibit very short distances, with V1-O10-V2 and V1-O11-V2 bond angles of 91.82 and 92.98°, which may make the magnetic orbitals nearly orthogonal.[29] Therefore, a ferromagnetic coupling contribution can be observed at low temperature for **3**.

Thermogravimetric analyses (TGA): TGA was carried out under an air flow with a heating rate of 10 °C min^{-1} in the temperature range 30–1000 °C (Figure S6, Supporting Information). Four distinct weight-loss stages are observed in the TG curve of **1**. The first stage, which occurs from 90 to 190 °C, is attributed to the loss of seven H_2O molecules (found 4.4 %, calcd 4.3 %). The remaining three stages occur between 90 and 728 °C, and are due to the loss of en molecules and the removal of the hydroxyl groups; the observed weight loss (14.5 %) is consistent with the calculated value (14.9 %). Later, a weight increase is observed in the region 728–756 °C, which is attributed to oxidation of V^{4+} to V^{5+}.[21,30] The residue may be a complex mixture of CdO, V_2O_5, and GeO_2; the observed residual weight (84.1 %) is in agreement with the calculated value (83.7 %). For **2**, three successive weight losses of 23.4 % (calcd 24.7 %) from 38 to 578 °C were attributed to removal of water molecules and dap molecules. A very complex process was observed from 578 to 730 °C for **2**, which includes the weight loss and weight increase attributed to removal of the volatile germanium oxide phase[23,31] and oxidation of V^{4+} to V^{5+}, respectively.[21,30] The residue may be a complex mixture of ZnO, V_2O_5, and GeO_2; the observed residual weight (77.3 %) is less than the calculated value (79.1 %), and further confirms the loss of the volatile germanium oxide phase in this process. For **3**, three successive weight losses of 20.3 % (calcd 20.1 %) from 50 to 707 °C, were attributed to the removal of water molecules, the hydroxyl groups, and dien molecules. Subsequently, a weight increase is observed in the region 707–802 °C, which is attributed to oxidation of the V^{4+} to V^{5+}.[21,30] The residue may be a complex mixture of CdO, V_2O_5, and GeO_2; the observed residual weight (84.5 %) is consistent with the calculated value (84.0 %).

Conclusion

We have successfully introduced GeO_4 tetrahedra into a polyoxovanadate cluster backbone to obtain novel extended hybrid heteropolyoxovanadates under hydrothermal conditions. These cluster anions are derived from the $\{V_{18}O_{42}\}$ shell by substitution of 2, 3, and 4 VO_5 square pyramids by Ge_2O_7 groups. Although discrete $[Ge_{2n}V_{18-n}O_{42}(O,OH)_n]$ ($n=2$, 4) clusters have been reported,[13,7g] the $[Ge_6V_{15}O_{48}]$ ($n=3$) cluster in **2** was first reported here. Furthermore, the inorganic–organic hybrid $[(en)_2Cd_2Ge_8V_{12}O_{40}(OH)_8]$ cluster in **1** is a rare example of Ge–V–O cluster backbone incorporating a third metal heteroatom. Compound **1** is an unique example of 1D vanadogermanate chain based on linkage of $[(en)_2Cd_2Ge_8V_{12}O_{40}(OH)_8]$ clusters and mononuclear bridging $[Cd(en)_2]$ groups. Compound **2** is the first example of a 2D vanadogermanate layer constructed from the $[Ge_6V_{15}O_{48}]$ cluster units and two types of TMC bridges including mononuclear [Zn(dap)] and dinuclear $[Zn_2(dap)_3]$ groups. Compound **3** is an unprecedented 3D framework built up from $[Ge_4V_{16}O_{42}(OH)_4]$ cluster units and unusual trinuclear bridging $[Cd_3(\mu\text{-dien})_2(Hdien)_2(H_2O)_2]$ groups.

These results emphasize the potential of Ge–V–O or TM-substituted Ge–V–O clusters and different TMCs as structural building units and bridging groups for constructing new materials and also demonstrate that hydrothermal techniques are a vital tool for materials design. Linking discrete Ge–V–O cluster units to make solid-state materials is of great interest not only from a structural point of view, but also from potential applications in different areas. Further work is in progress.

Experimental Section

Chemicals, reagents, and analyses: All chemicals were used as purchased without purification. Elemental analyses (C, H, and N) were performed on a PE2400 II elemental analyzer. Energy-dispersive X-ray analysis (EDXA) was performed with a JEOL-JSM-6700F field emission scanning electron microscope. The IR spectra were obtained on an ABB Bomen MB 102 spectrometer in the range of 4000–400 cm^{-1} with pressed KBr pellets. Thermogravimetric analyses (TGA) were performed on a Mettler TGA/SDTA851 thermal analyzer under an air flow with a heating rate of 10 °C min^{-1} in the temperature region of 30–1000 °C. Variable-temperature magnetic susceptibility measurements were carried out in the temperature range of 2–300 K with a Quantum Design MPMS-XL5 SQUID magnetometer. The magnetic data were corrected for the diamagnetic contribution of the sample holder and the diamagnetic contribution of the sample by using Pascal constants.

Synthesis of $\{(en)_2Cd_2Ge_8V_{12}O_{40}(OH)_8[Cd(en)_2]_2(H_2O)\}\cdot 6H_2O$ (1): A mixture of GeO_2 (0.1040 g, 1 mmol), NH_4VO_3 (0.2340 g, 2 mmol), $CdCl_2\cdot 2.5H_2O$ (0.1440 g, 0.5 mmol), H_3BO_3 (0.061 g, 1 mmol), en (0.5 mL), and H_2O (5 mL) was stirred for 2 h, sealed in a Teflon-lined steel autoclave (pH 10, 20 mL), kept at 170 °C for 5 d, and then cooled to RT. Dark block crystals were obtained by filtration, washed with distilled water, and dried in air (yield: ca. 80% based on GeO_2). **1** was also prepared by replacing NH_4VO_3 with V_2O_5 under the same conditions. IR (KBr pellet): $\tilde{\nu}$ = 3436 (m), 3331 (m), 2939 (vw), 2881 (vw), 1598 (m), 1464 (w), 1388 (w), 976 (s), 784 (vs), 727 (m), 670 (m), 536 cm^{-1} (s); elemental analysis calcd (%) for $C_{12}H_{70}Cd_4Ge_8N_{12}O_{55}V_{12}$: C 4.96, H 2.43, N 5.79; found: C 5.17, H 2.40, N 5.90.

Synthesis of $\{[Zn_2(dap)_3][Zn(dap)]_2Ge_6V_{15}O_{48}(H_2O)\}[Zn(dap)_2(H_2O)]_2\cdot 3H_2O$ (2): A mixture of GeO_2 (0.0104 g, 0.1 mmol), V_2O_5 (0.0364 g, 0.2 mmol), $ZnSO_4$ (0.0721 g, 0.25 mmol), dap (0.5 mL) and H_2O (5 mL) was stirred for 0.5 h, sealed in a Teflon-lined steel autoclave (pH 12, 20 mL), kept at 170 °C for 3 d, and then cooled to RT. Brown block crystals were obtained by filtration, washed with distilled water, and dried in air (yield: ca. 78% based on GeO_2). IR (KBr pellet): $\tilde{\nu}$ = 3301 (m), 3258 (m), 2950 (w), 2873 (w), 1579 (m), 1451 (w), 1391 (w), 1185 (w), 1023 (m), 972 (vs), 800 (vs), 766 (vs), 680 (s), 637 (s), 587 cm^{-1} (s), elemental analysis calcd (%) for $C_{27}H_{102}Ge_6N_{18}O_{54}V_{15}Zn_6$: C 10.34, H 3.28, N 8.04; found: C 10.26, H 3.30, N 7.96.

Synthesis of $\{[Cd_3(\mu\text{-dien})_2(Hdien)_2(H_2O)_2]Ge_4V_{16}O_{42}(OH)_4(H_2O)\}\cdot 2H_2O$ (3): A mixture of GeO_2 (0.1040 g, 0.1 mmol), V_2O_5 (0.3250 g, 1.7 mmol), $CdCl_2\cdot 2.5H_2O$ (0.1140 g, 0.5 mmol), dien (0.5 mL), ethylene glycol (pH 9, 2 mL), and H_2O (10 mL) was stirred for 0.2 h, sealed in a Teflon-lined steel autoclave (20 mL), kept at 170 °C for 3 d, and then cooled to RT. Dark block crystals were obtained by filtration, washed with distilled water, and dried in air (yield: ca. 90% based on GeO_2). IR (KBr pellet): $\tilde{\nu}$ = 3316 (m), 3231 (m), 3154 (m), 2930 (w), 2879 (w), 1583 (m), 1506 (m), 1447 (m), 1361 (w), 1231 (w), 1180 (w), 1112 (w), 965 (vs), 820 (s), 743(s), 683 (vs), 596 cm^{-1} (s). Elemental analysis (%) calcd for $C_{16}H_{68}Cd_3Ge_4N_{12}O_{51}V_{16}$: C 7.12, H 2.54, N 6.23; found: C 7.30, H 2.39, N 6.30;

X-ray crystallography: The intensity data sets were collected by using a Rigaku Mercury CCD with graphite-monochromated $Mo_{K\alpha}$ radiation (λ = 0.71073 Å) in the ω scanning mode at RT. All absorption corrections were performed with the multi-scan program. The structures were solved by direct methods and refined by full-matrix least-squares techniques on F^2 with the SHELXTL-97 program.[32] All atoms except for H atoms were refined anisotropically. No H atoms associated with free water molecules were located from the difference Fourier map. The H atoms of the organic ligands, except for the C2, C13, N6, N7, N8, and N9 atoms in **2** and the C3, C4, and N3 atoms in **3**, were geometrically placed and refined by using a riding model. For **2**, O1w, N6, N7, N8, and Zn4 atoms were disordered over two positions (Figure S7, Supporting Information) with occupation factors of 0.70 and 0.30. In addition, the C1 atoms in **2** have occupancies of 0.5. Such disorder has also been previously observed.[20c] For **3**, the C4 atom was also disordered over two positions with occupation factors of 0.70 and 0.30. Further details of the structural analyses of **1**–**3** are summarized in Table 1. The ranges of some important bond lengths of **1**–**3** are listed in Table S1 (Supporting Information). CCDC 747777 (**1**), 747778 (**2**) and 747779 (**3**) contain the supplementary crystallographic data for this paper. These data can be obtained free of charge from The Cambridge Crystallographic Data Centre via www.ccdc.cam.ac.uk/data request/cif.

Acknowledgements

This work was supported by the National Natural Science Fund of China (no. 50872133), the NNSF for Distinguished Young Scholars of China (no. 20725101), the 973 Program (no. 2006CB932904), the NSF of Fujian Province (no. E0510030) and the NNSF of China (no. 20821061). This project was also supported by China Postdoctoral Science Foundation (no. 20090450183).

Table 1. X-ray crystallographic data for **1**–**3**.

	1	**2**	**3**
formula	$C_{12}H_{70}Cd_4Ge_8N_{12}O_{55}V_{12}$	$C_{27}H_{102}Ge_6N_{18}O_{54}V_{15}Zn_6$	$C_{16}H_{68}Cd_3Ge_4N_{12}O_{51}V_{16}$
M_r	2904.39	3135.14	2687.42
crystal system	monoclinic	orthorhombic	monoclinic
space group	$C2/c$	$C222_1$	$C2/c$
Z	4	4	4
T [K]	293(2)	293(2)	293(2)
a [Å]	15.262(3)	13.355(3)	21.388(4)
b [Å]	19.834(4)	25.692(5)	13.272(3)
c [Å]	23.991(5)	29.379(6)	24.344(5)
β [°]	95.27(3)	90	100.96(3)
V [Å^3]	7232(3)	10081(4)	6784(2)
ρ_{calcd} [g cm^{-1}]	2.655	2.040	2.622
μ [mm^{-1}]	5.995	4.559	4.857
reflns collected	24982	24499	21007
unique reflns (R_{int})	6419 (0.0359)	8644 (0.0729)	6013 (0.0216)
refined parameters	480	628	479
R_1[a]/wR_2[b] [$I > 2\sigma(I)$]	0.0256/0.0646	0.0663/0.1723	0.0292/0.0767
R_1[a]/wR_2[b](all data)	0.0302/0.0668	0.0879/0.2107	0.0302/0.0775
largest diff. peak/hole [e Å^{-3}]	1.015/−0.681	1.529/−1.599	1.851/−0.707

[a] $R_1 = \Sigma||F_o| - |F_c||/\Sigma|F_o|$. [b] $wR_2 = [\Sigma w(F_o^2 - F_c^2)^2/\Sigma w(F_o^2)^2]^{1/2}$; $w = 1/[\sigma^2(F_o^2) + (xP)^2 + yP]$, $P = (F_o^2 + 2F_c^2)/3$, in which x = 0.0359, y = 4.5636 for **1**; x = 0.1170, y = 118.4627 for **2**; x = 0.0406, y = 52.2854 for **3**.

[1] a) N. Mizuno, K. Yamaguchi, K. Kamata, *Coord. Chem. Rev.* **2005**, *249*, 1944–1956; b) D. A. Judd, J. H. Nettles, N. Nevins, J. P. Snyder, D. C. Liotta, J. Tang, J. Ermolieff, R. F. Schinazi, C. L. Hill, *J. Am. Chem. Soc.* **2001**, *123*, 886–897; c) A. Müller, P. Kögerler, A. W. M. Dress, *Coord. Chem. Rev.* **2001**, *222*, 193–218; d) H. Tan, Y. Li, Z. Zhang, C. Qin, X. Wang, E. Wang, Z. Su, *J. Am. Chem. Soc.* **2007**, *129*, 10066–10067; e) C. Pichon, A. Dolbecq, P. Mialane, J. Marrot, E. Rivière, M. Goral, M. Zynek, T. McCormac, S. A. Borshch, E. Zueva, F. Sécheresse, *Chem. Eur. J.* **2008**, *14*, 3189–3199; f) A. Giusti, G. Charron, S. Mazerat, J. Compain, P. Mialane, A. Dolbecq, E. Rivière, W. Wernsdorfer, R. N. Biboum, B. Keita, L. Nadjo, A. Filoramo, J. Bourgoin, T. Mallah, *Angew. Chem.* **2009**, *121*, 5049–5052; *Angew. Chem. Int. Ed.* **2009**, *48*, 4949–4952.

[2] a) D.-L. Long, C. Streb, Y.-F. Song, S. Mitchell, L. Cronin, *J. Am. Chem. Soc.* **2008**, *130*, 1830–1832; b) A. Yoshida, Y. Nakagawa, K. Uehara, S. Hikichi, N. Mizuno, *Angew. Chem.* **2009**, *121*, 7189–7192; *Angew. Chem. Int. Ed.* **2009**, *48*, 7055–7058; c) K. Micoine, B. Hasenknopf, S. Thorimbert, E. Lacôte, M. Malacria, *Angew. Chem.* **2009**, *121*, 3518–3520; *Angew. Chem. Int. Ed.* **2009**, *48*, 3466–3468.

[3] a) M. Wei, C. He, Q. Sun, Q. Meng, C. Duan, *Inorg. Chem.* **2007**, *46*, 5957–5966; b) J. Niu, Q. Wu, J. Wang, *J. Chem. Soc. Dalton Trans.* **2002**, 2512–2516; c) J. Sha, J. Peng, A. Tian, H. Liu, J. Chen, P. Zhang, Z. Su, *Cryst. Growth Des.* **2007**, *7*, 2535–2541; d) A. Müller, V. P. Fedin, C. Kuhlmann, H. Bögge, B. Hauptfleisch, V. P. Fedin, H. Fenske, G. Baum, *Chem. Commun.* **1999**, 1189–1190; e) J. M. Knaust, C. Inman, S. W. Keller, *Chem. Commun.* **2004**, 492–493; f) Y. Ishii, Y. Takenaka, K. Konishi, *Angew. Chem.* **2004**, *116*, 2756–2759; *Angew. Chem. Int. Ed.* **2004**, *43*, 2702–2705.

[4] a) J.-W. Zhao, H.-P. Jia, J. Zhang, S.-T. Zheng, G.-Y. Yang, *Chem. Eur. J.* **2007**, *13*, 10030–10045; b) J.-W. Zhao, C.-M. Wang, J. Zhang, S.-T. Zheng, G.-Y. Yang, *Chem. Eur. J.* **2008**, *14*, 9223–9239; c) L. San Felices, P. Vitoria, J. M. Gutiérrez-Zorrilla, S. Reinoso, J. Etxebarria, L. Lezama, *Chem. Eur. J.* **2004**, *10*, 5138–5146; d) C.-M. Liu, D.-Q. Zhang, M. Xiong, D.-B. Zhu, *Chem. Commun.* **2002**, 1416–1417.

[5] S.-T. Zheng, J. Zhang, G.-Y. Yang, *Inorg. Chem.* **2005**, *44*, 2426–2430.

[6] Z. Zhang, Y. Li, Y. Wang, Y. Qi, E. Wang, *Inorg. Chem.* **2008**, *47*, 7615–7622.

[7] a) A. Müller, J. Döring, *Angew. Chem.* **1988**, *100*, 1789–1789; *Angew. Chem. Int. Ed. Engl.* **1988**, *27*, 1721–1722; b) G. Huan, M. A. Greaney, A. J. Jacobson, *J. Chem. Soc. Chem. Commun.* **1991**, 260–261; c) D. Gatteschi, B. Tsukerblat, A. L. Barra, L. C. Brunel, A. Müller, J. Döring, *Inorg. Chem.* **1993**, *32*, 2114–2117; d) R. Basler, G. Chaboussant, A. Sieber, H. Andres, M. Murrie, P. Kögerler, H. Bögge, D. C. Crans, E. Krickemeyer, S. Janssen, H. Mutka, A. Müller, H. U. Gudel, *Inorg. Chem.* **2002**, *41*, 5675–5685; e) A. Tripathi, T. Hughbanks, A. Clearfield, *J. Am. Chem. Soc.* **2003**, *125*, 10528–10529; f) X. Wang, L. Liu, G. Zhang, A. J. Jacobson, *Chem. Commun.* **2001**, 2472–2473; g) D. Pitzschke, J. Wang, R.-D. Hoffmann, R. Pöttgen, W. Bensch, *Angew. Chem.* **2006**, *118*, 1327–1331; *Angew. Chem. Int. Ed.* **2006**, *45*, 1305–1308.

[8] B. Dong, J. Peng, C. J. Gómez-García, S. Benmansour, H. Jia, N. Hu, *Inorg. Chem.* **2007**, *46*, 5933–5941.

[9] Y. Qi, Y. Li, E. Wang, H. Jin, Z. Zhang, X. Wang, S. Chang, *Inorg. Chim. Acta* **2007**, *360*, 1841–1853.

[10] R. Kiebach, C. Näther, P. Kögerlerb, W. Bensch, *Dalton Trans.* **2007**, 3221–3223.

[11] R. Kiebach, C. Näther, W. Bensch, *Solid State Sci.* **2006**, *8*, 964–970.

[12] a) X.-B. Cui, J.-Q. Xu, Y. Li, Y.-H. Sun, G.-Y. Yang, *Eur. J. Inorg. Chem.* **2004**, 1051–1055; b) S.-T. Zheng, J. Zhang, J.-Q. Xu, G.-Y. Yang, *J. Solid State Chem.* **2005**, *178*, 3740–3746; c) S.-T. Zheng, Y.-M. Chen, J. Zhang, J.-Q. Xu, G.-Y. Yang, *Eur. J. Inorg. Chem.* **2006**, 397–406.

[13] T. Whitfield, X. Wang, A. J. Jacobson, *Inorg. Chem.* **2003**, *42*, 3728–3733.

[14] a) S.-T. Zheng, J. Zhang, G.-Y. Yang, *Angew. Chem.* **2008**, *120*, 3973–3977; *Angew. Chem. Int. Ed.* **2008**, *47*, 3909–3913; b) S.-T. Zheng, D.-Q. Yuan, H.-P. Jia, J. Zhang, G.-Y. Yang, *Chem. Commun.* **2007**, 1858–1860; c) R. C. Howell, F. G. Perez, S. Jain, W. D. Horrocks, A. L. Rheingold, L. C. Francesconi, *Angew. Chem.* **2001**, *113*, 4155–4158; *Angew. Chem. Int. Ed.* **2001**, *40*, 4031–4034; d) F. Hussain, B. S. Bassil, L.-H. Bi, M. Reicke, U. Kortz, *Angew. Chem.* **2004**, *116*, 3567–3571; *Angew. Chem. Int. Ed.* **2004**, *43*, 3485–3488; e) S. S. Mal, U. Kortz, *Angew. Chem.* **2005**, *117*, 3843–3846; *Angew. Chem. Int. Ed.* **2005**, *44*, 3777–3780.

[15] a) X.-B. Cui, J.-Q. Xu, H. Meng, S.-T. Zheng, G.-Y. Yang, *Inorg. Chem.* **2004**, *43*, 8005–8009; b) S.-T. Zheng, M.-H. Wang, G.-Y. Yang, *Inorg. Chem.* **2007**, *46*, 9503–9508.

[16] a) Y. Qi, Y. Li, C. Qin, E. Wang, H. Jin, D. Xiao, X. Wang, S. Chang, *Inorg. Chem.* **2007**, *46*, 3217–3230; b) Y. Qi, Y. Li, E. Wang, Z. Zhang, S. Chang, *Dalton Trans.* **2008**, 2335–2345.

[17] a) R. L. LaDuca, Jr, R. S. Rarig, Jr, P. J. Zapf, J. Zubieta, *Inorg. Chim. Acta* **1999**, *292*, 131–136; b) C.-M. Liu, D.-Q. Zhang, D.-B. Zhu, *Cryst. Growth Des.* **2003**, *3*, 363–368; c) N. Snejko, M. E. Medina, E. Gutierrez-Puebla, M. A. Monge, *Inorg. Chem.* **2006**, *45*, 1591–1594; d) C.-M. Liu, D.-Q. Zhang, D.-B. Zhu, *Cryst. Growth Des.* **2005**, *5*, 1639–1642.

[18] I. D. Brown, D. Altermatt, *Acta Crystallogr.* **1985**, B41, 244–247.

[19] S. Hu, Z. Zhou, K. Tsai, *Acta Phys. Chim. Sin.* **2003**, 19, 1073–1077.

[20] a) S.-T. Zheng, M.-H. Wang, G.-Y. Yang, *Chem. Asian J.* **2007**, *2*, 1380–1387; b) Y. Xu, L.-B. Nie, D. Zhu, Y. Song, G.-P. Zhou, W.-S. You, *Cryst. Growth Des.* **2007**, *7*, 925–929; c) Z. Shi, L. Zhang, G. Zhu, G. Yang, J. Hua, H. Ding, S. Feng, *Chem. Mater.* **1999**, *11*, 3565–3570; d) Z. Zhang, J. Liu, E. Wang, C. Qin, Y. Li, Y. Qi, X. Wang, *Dalton Trans.* **2008**, 463–468.

[21] J. Zhou, S.-T. Zheng, W.-H. Fang, G.-Y. Yang, *Eur. J. Inorg. Chem.* **2009**, 5075–5078.

[22] J. Zhou, G.-Q. Bian, Y. Zhang, Q.-Y. Zhu, C.-Y. Li, J. Dai, *Inorg. Chem.* **2007**, *46*, 6347–6352.

[23] H.-X. Zhang, J. Zhang, S.-T. Zheng, G.-Y. Yang, *Inorg. Chem.* **2003**, *42*, 6595–6597.

[24] D. Jia, Y. Zhang, Q. Zhao, J. Deng, *Inorg. Chem.* **2006**, *45*, 9812–9817.

[25] S.-T. Zheng, J. Zhang, B. Li, G.-Y. Yang, *Dalton Trans.* **2008**, 5584–5587.

[26] M. I. Khan, E. Yohannes, R. J. Doedens, *Inorg. Chem.* **2003**, *42*, 3125–3129.

[27] J. Zhou, Y. Zhang, G.-Q. Bian, Q.-Y. Zhu, C.-Y. Li, J. Dai, *Cryst. Growth Des.* **2007**, *7*, 1889–1892.

[28] a) S. Mukherjee, Y. Lan, G. E. Kostakis, R. Clérac, C. E. Anson, A. K. Powell, *Cryst. Growth Des.* **2009**, *9*, 577–585; b) M.-H. Zeng, M.-C. Wu, H. Liang, Y.-L. Zhou, X.-M. Chen, S.-W. Ng, *Inorg. Chem.* **2007**, *46*, 7241–7243; c) J. I. Kim, H. S. Yoo, E. K. Koh, H. C. Kim, C. S. Hong, *Inorg. Chem.* **2007**, *46*, 8481–8483.

[29] a) A. C. Komarek, T. Taetz. T, M. T. Fernández-Díaz, D. M. Trots, A. Möller, M. Braden, *Phys. Rev. B* **2009**, *79*, 104425; b) W. Geertsma, D. Khomakii, *Phys. Rev. B* **1999**, *54*, 3011, and references therein.

[30] S.-T. Zheng, Y.-M. Chen, J. Zhang, G.-Y. Yang, *Z. Anorg. Allg. Chem.* **2006**, 632, 155–159.

[31] N. N. Julius, A. Choudhury, C. N. R. Rao, *J. Solid State Chem.* **2003**, *170*, 124–129.

[32] a) G. M. Sheldrick, SHELXS97, Program for Crystal Structure Solution, University of Göttingen, Göttingen (Germany), **1997**; b) G. M. Sheldrick, SHELXL97, Program for Crystal Structure Refinement, University of Göttingen, Göttingen (Germany), **1997**.

Received: May 24, 2010
Published online: October 4, 2010

